Supplementary Information (SI) for Chemical Communications.
This journal is © The Royal Society of Chemistry 2024

Solid-State Synthesis of Ligand-Assisted Lead Halide Nanoclusters

*David C. Zeitz, Kai-Chun Chou, and Jin Z. Zhang**

Department of Chemistry and Biochemistry, University of California, Santa Cruz, CA 95064, USA

* Corresponding Author. Email: zhang@ucsc.edu

EXPERIMENTAL METHODS

Materials

Butyric acid (BTA) 99.5%, oleylamine (OAm) 70% tech. grade, toluene 99%, methylammonium bromide (MABr) 98%, and lead bromide ($PbBr_2$) 98%+ were purchased from Sigma-Aldrich. Octanoic acid (OCA) 99% and n-octylamine (OCAm) 99% were purchased from Acros Organics. N, N-Dimethylformamide (DMF) was purchased from Oakwood Chemical, butylamine (BTYA) 99% from TCI Chemicals, and oleic acid (OA) from Fisher Scientific. All chemicals were used as received with no further processing or purification.

Synthesis of $PbBr_2$-OA-OAm PMSCs in solid state

The PMSC synthetic scheme proposed follows a solid-state approach, where 0.080 mmol, 9.0 mg and 29.3 mg, respectively, of MABr and $PbBr_2$ were added to an agate mortar and ground for five minutes, yielding an orange product with green luminescence under a 365 nm UV lamp. 0.300 mmol (94 µL) of OA was then added and ground with the metal halide precursors for five minutes. Last, 0.300 mmol (100 µL) of OAm was added and ground for an additional five minutes, yielding an orange product with a mixture of green and dark blue luminescence. The prepared product was then suspended in 20.00 mL of toluene, followed by centrifugation at 5000 rpm for five minutes

to remove excess suspended solids. The dark blue luminescing supernatant was retained for optical characterization.

Synthesis of $PbBr_2$-BTA-BTYA MHMCs in solid state

The BTA and BTYA passivated MHMCs scheme is like that of PMCSs, but without MABr. 0.200 mmol (73.0 mg) of $PbBr_2$ was added to an agate mortar with 2.00 mmol (183 μL) of butyric acid (BTA) and ground for five minutes. Next, 2.00 mmol (198 μL) of butylamine was added and ground for an additional five minutes, yielding a white product with dark blue luminescence. The prepared product was then suspended in 5.00 mL of toluene followed by further dilution at a rate of 1.00 mL product to 5.00 mL toluene, where the diluted colloid was retained for optical characterization.

Synthesis of $PbBr_2$-BTYA MHMCs in solid state

Synthesis proceeded as above for BTA and BTYA passivated MHMCs but without the addition of BTA and with the removal of the corresponding grinding step. 0.200 mmol (73.0 mg) of $PbBr_2$ was added to an agate mortar with 2.00 mmol (198 μL) of butylamine was added and ground for five minutes, yielding a white product with dark blue luminescence. The prepared product was then suspended in 5.00 mL of toluene followed by further dilution at a rate of 1.00 mL product to 5.00 mL toluene, where the diluted colloid was retained for optical characterization.

Synthesis of $PbBr_2$-OA-OAm PMSCs in solution state

0.080 mmol of MABr and $PbBr_2$ (9.0 and 29.3 mg) were dissolved by vortex in 400 μL DMF. 0.300 mmol (94 μL) of OA was injected rapidly and dissolved by vortex. Once homogeneous,

0.300 mmol (100 μL) OAm was injected rapidly and dissolved by vortex to complete preparation of the precursor solution. 100 μL of precursor was rapidly injected into 5.00 mL of toluene under magnetic stirring at 1150 rpm, yielding a pale-yellow solution with deep blue luminescence under a 365 nm UV lamp. The colloid was centrifuged at 5000 rpm for 5 minutes to remove excess suspended solids and the supernatant was retained for optical characterization.

Synthesis of $PbBr_2$-BTA-BTYA MHMCs in solution state

0.200 mmol of $PbBr_2$ (73.0 mg) was dissolved by vortex in 400 μL DMF. 2.00 mmol (183 μL) of BTA was injected rapidly and dissolved by vortex. Once homogeneous, 2.00 mmol (198 μL) OAm was injected rapidly and dissolved by vortex to complete preparation of the precursor solution. 100 μL of precursor was rapidly injected into 5.00 mL of toluene under magnetic stirring at 1150 rpm. 1.00 mL of this solution was injected to an additional 5.00 mL of toluene under magnetic stirring at 1150 rpm and retained for optical characterization.

Purification of solid state BTYA MHMCs

After grinding, the residual ligand was allowed to dry before the crude product was resuspended in toluene with an additional 2.00 mmol aliquot of BTYA at a rate of 0.6 mg/mL and sonicated until homogeneous. The suspended product was turbid and displayed no luminescence under irradiation by a 365 nm lamp. The suspended MHMCs were diluted at a rate of 20 μL/mL in toluene, forming a clear, deep blue emitting colloid. The purified MHMCs were removed from the colloid by centrifuging at 10,000 rpm for 5 minutes and retaining the pellet.

Spectroscopic measurements

UV-vis absorption was measured with an Agilent Technologies Cary 60 UV-Vis spectrophotometer. Photoluminescence was measured using an Agilent Technologies Cary Eclipse Fluorescence Spectrophotometer.

Raman spectra were obtained using a Thermo Fisher DXR3 Raman Microscope with a 785 nm excitation laser at 10 mW power. For MHMC, the sample was prepared by compressing the prepared BTYA-passivated MHMC powder into a pellet and was measured on a stainless-steel substrate for a 5.00 s exposure time for 10 exposures. For PMSC, the colloid was drop cast onto a stainless-steel substrate and data was immediately acquired. A 50x objective was used for focusing and the spectrograph aperture was a 50 μm pinhole.

Time-resolved photoluminescence (TRPL) was conducted using a Light Conversion laser system. The pump beam was generated by a ytterbium-doped potassium gadolinium tungstate (Yb:KGW) lasing medium (PHAROS, Light Conversion) with an output of 1030 nm, a power of of 10 W, and a 20 kHz repetition rate. 80% of the fundamental beam was routed through an optical parametric amplifier (ORPHEUS, Light Conversion) to produce tunable pump wavelengths. A nonlinear second harmonic generating unit (LYRA, Light Conversion) was used to select a pump wavelength of 370 nm. A 400 nm long pass filter was used to eliminate the pump beam following excitation. Data was acquired at minimum pump power, using a 10 s collection time, recorded using a photomultiplier tube affixed to an Oxford Instruments Andor Kymera spectrometer, and using the corresponding HARPIA service app data acquisition software. The data was processed

using Igor64 and was fit using the double exponential fit function $f(x) = y_0 + A_1*\exp(-x/t_1) + A_2*\exp(-x/t_2)$.

XRD measurements

The MHMC sample was analyzed as a powder which was finely ground before measuring. X-ray diffraction (XRD) was collected on a Rigaku Smartlab Powder and Thin Film Diffractometer at 0.02 degrees per step and 1 dpm, at 2θ angles ranging from 2 to 40°. The PMSCs sample was prepared by dissolving 48.0 mg paraffin in 20.00 mL of the PMSC solution. Then, the solution was spun down by centrifuge at a speed of 12500 rpm for 30 minutes. The resultant pellet was applied directly to a microscope slide and stored under vacuum until characterization at 0.05 dpm with a step size of 0.02.

TEM measurements

The MHMC sample was prepared as described above and suspended in 5.00 mL of toluene. 1.00 mL of the suspension was further diluted in 5.00 mL of hexane and centrifuged at 500 rpm for five minutes to remove any remaining large aggregates. The supernatant was extracted and drop cast onto hexagonal, 400 mesh copper grids with carbon support film of standard 3-4 nm thickness (Electron Microscopy Sciences, CF400H-Cu-UL). The grids were dried in a desiccator under vacuum for 6 hours before being removed to ambient conditions for analysis. HRTEM was performed at the National Center for Electron Microscopy (NCEM) at the Lawrence Berkeley National Laboratory Molecular Foundry on an FEI UT Tecnai microscope operated at a 200 kV acceleration voltage. The images were analyzed with ImageJ.

EXPERIMENTAL RESULTS

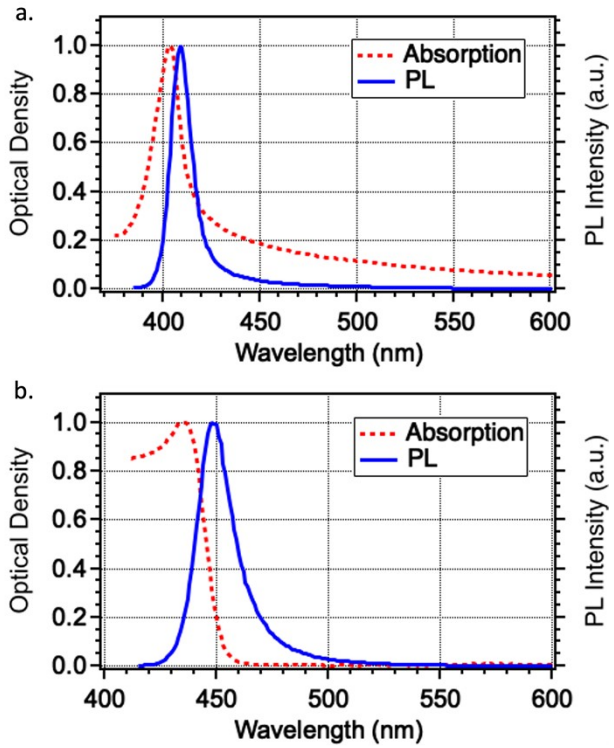

Figure S1 UV-Vis electronic absorption and photoluminescence (PL) spectra of (a) LARP synthesized MHMCs with excitation at 365 nm, and (b) LARP PMSCs with excitation at 400 nm.

To make a direct comparison between LARP and solid-state MHMCs and PMSCs, each particle was synthesized using identical precursor and ligand concentrations as the solid-state particles. Figure S1a shows normalized absorption and emission spectra of the LARP MHMCs peaked at 404 and 409 nm respectively. These peak positions are coincident with those seen in the solid-state synthesis. Similarly, Figure S1b shows normalized absorption and emission spectra with featured absorption and emission peaks at 435 nm and 448 nm, respectively. This represents a 3 nm difference in peak position in comparison to that of the solid-state synthesis.

To test the veracity of the PMSC solid-state method, 0.300 mmol (47.0 and 50.0 μL) of OCA and OCAm were used in place of OA and OAm. PMSCs were formed with first excitonic absorption and emission recorded at 425 and 433 nm respectively. The PMSCs passivated with OCA and OCAm as shown in Figure S2 are slightly blue shifted but have a similarly narrow PL FWHM of 15 nm compared with the OA OAm PMSCs.

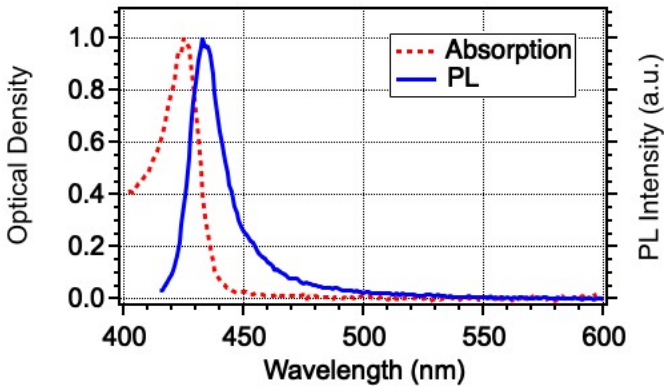

Figure S2 The first excitonic absorption and corresponding emission peaks of the solid-state MHMCs synthesized using OCA and OCAm as passivating ligands. The PL band was measured following excitation at 365 nm.

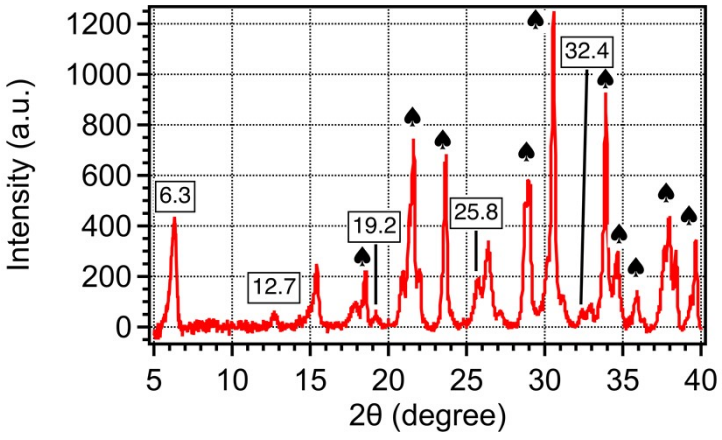

Figure S3 XRD of crude BTYA-passivated MHMC powders. The numbered peaks are associated with the MHMC product, while the peaks marked by spades are associated with $PbBr_2$ precursor. MHMC product was compared against COD card number 1010619.[1]

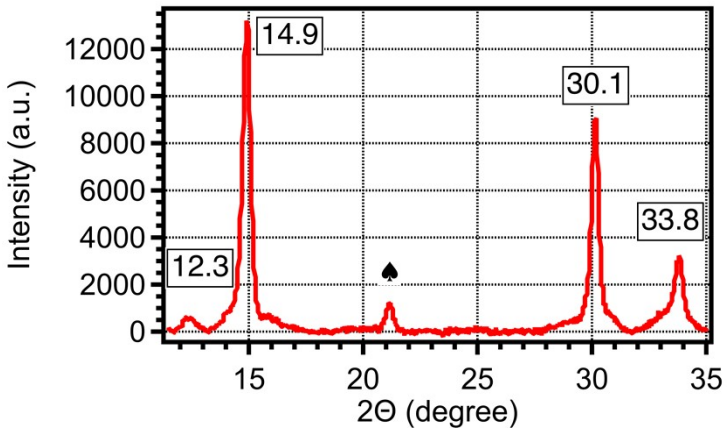

Figure S4 XRD of the solid state synthesized PMSC sample. The peak marked with the spade is associated with the paraffin stabilizing matrix.

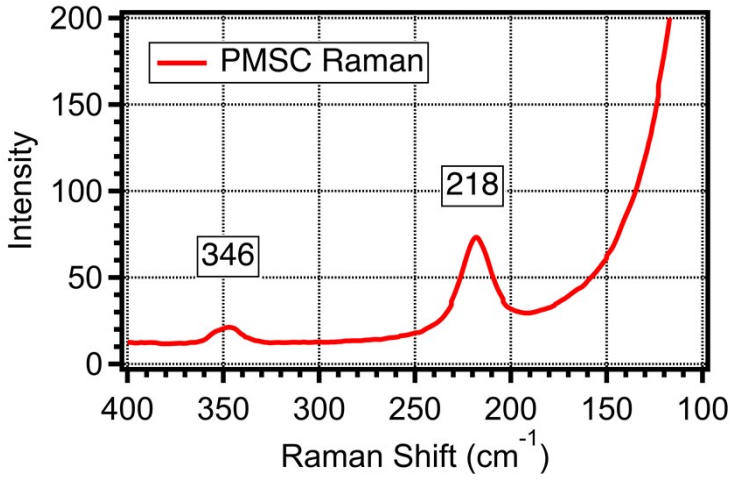

Figure S5 Raman spectrum of the liquid PMSC sample synthesized in the solid state.

To verify that no $PbBr_2$ clusters could form with coincident absorption and emission features as the ligand passivated MHMCs, 0.200 mmol (73.0 mg) $PbBr_2$ was ground down without ligand and dispersed as described in the synthesis of MHMCs described above. No sharp optical features were

observed. This supports the assertion that the presence of ligand (particularly the amine) is necessary for the formation of MHMCs. To assess the stability of the solid-state synthesized MHMCs, a stability test was carried out. Particles were synthesized as described above, and the absorbance was measured by transmission through a thin layer of MHMCs applied to a glass microscope slide. The slide was precleaned by soaking in detergent, followed by a triple rinse in DI water, followed by soaking in acetone. Figure S2 shows the absorbance as measured shortly after synthesis, then on the fourteenth and thirty fifth days. The absorbance data are presented as raw data (a), and as normalized data (b) to better visualize the minor difference in the peak position over time.

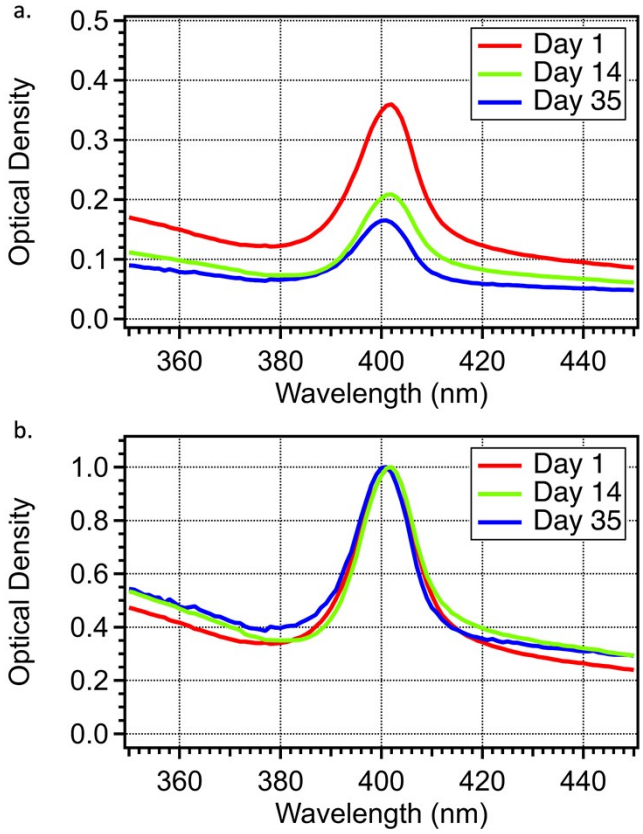

Figure S6 The first excitonic absorption peaks of the solid-state MHMCs measured over 35 days, with both raw (a), and normalized presentation (b).

Table S1 Raman band assignments for BTYA passivated MHMCs synthesized in the solid state

Raman Shift (cm^{-1})	Assignment
58	Octahedral distortion
74	BTYA lurching
87	BTYA lurching
104	BTYA lurching
260	C-N torsion
322	C-N torsion

References

(1) Vaitkus, A.; Merkys, A.; Sander, T.; Quirós, M.; Thiessen, P. A.; Bolton, E. E.; Gražulis, S. A Workflow for Deriving Chemical Entities from Crystallographic Data and Its Application to the Crystallography Open Database. *Journal of Cheminformatics* **2023**, *15* (1), 123. https://doi.org/10.1186/s13321-023-00780-2.

(2) Wang, K.-H.; Li, L.-C.; Shellaiah, M.; Wen Sun, K. Structural and Photophysical Properties of Methylammonium Lead Tribromide (MAPbBr3) Single Crystals. *Sci Rep* **2017**, *7* (1), 13643. https://doi.org/10.1038/s41598-017-13571-1.

(3) Guarino-Hotz, M.; Barnett, J. L.; Chou, K.-C.; Win, A. A.; Zhang, H.; Song, C.; Oliver, S. R. J.; Zhang, J. Z. Structural Study of Paraffin-Stabilized Methylammonium Lead Bromide Magic-Sized Clusters. *J. Phys. Chem. C* **2023**, *127* (6), 3367–3376. https://doi.org/10.1021/acs.jpcc.2c08645.

(4) Mączka, M.; Ptak, M. Temperature-Dependent Raman Studies of FAPbBr3 and MAPbBr3 Perovskites: Effect of Phase Transitions on Molecular Dynamics and Lattice Distortion. *Solids* **2022**, *3* (1), 111–121. https://doi.org/10.3390/solids3010008.